



International Journal of Recent Development in Engineering and Technology
Website: www.ijrdet.com (ISSN 2347-6435(Online) Volume 10, Issue 8, August 2021)

Design and Simulation of High Frequency Solid State Transformer for Electric Locomotive Power Supply

Deepti Gautam¹, Parikshit Bajpai²

Abstract--With the construction of electrified railways in India, high-power electric locomotives and high-speed trains are applied, which greatly promotes the economic development. The electric traction technology based on power conversion and alternating current (AC) motor speed adjusting is one of the key technologies of electric locomotive and high-speed electric multiple units. So far, most of them have been applied maturely. The traction equipment with huge volume will limit the passenger capacity and make structural design of a train more difficult; additionally, the load of traction equipment will directly affect the acceleration and braking performances of a train, thus affecting the safe operation of the train and passenger comfort. In the traction system, the most traction transformer approximately accounts for 1/3 of the whole equipment. Multiple topologies adopting high frequency transformer (HFT) are suggested by scholars to scale back the quantity and weight of main transformer for train traction and to enhance the reliability and adaptability of traction system.

I. INTRODUCTION

The future locomotive traction system is also being planned to reduce or prevent the effects of power quality incidents (e.g., voltage dips), boost stability indices (e.g., by minimizing the amount and length of interruptions), and maximize performance (e.g., by reducing losses). The normal low frequency in power transformer of traction system is widely used. This is due to their low cost, high reliability, and high efficiency. But as always as there is advantages there is also some disadvantages the low frequency power transformer has few power quality issues like; the voltage drop in loading time, inability to mitigate flicker", sensitivity to harmonics, environmental concerns regarding mineral oil, limited performance under DC-offset load unbalances, and a need for protection of the primary system from problems arising inside or beyond the transformer. It is clear that the Power quality is an extremely important issue especially with utility end users; this is the fact that makes these problems more serious today than before. The solution was founded, when the concept of a solid-state transformer (SST) was mentioned as an alternative to the low frequency power transformer. At that time the successful demonstration of the concept wasn't so clear, however the advantages of this new concepts were clear. Nowadays with the recent advancements in the field of power electronics and semiconductors, and with the deep understanding of the multilevel converters, the concept became more viable.

The solid-state transformer is an essential part of locomotive traction power supply (SST). The SST applies additional functions to the traction power such as reactive power compensation, limited short-circuit currents, and voltage sag compensation, as well as new ways to regulate the energy routing. However, it should be noted that all of these features would come at the expense of a more sophisticated and costly framework. These topologies are intended to transform single-phase line frequency alternating current into a medium frequency alternating current, which is then connected to high frequency corrector and traction inverter by high frequency step-down transformers. This modern kind of converter topology is called a solid-state transformer (sSTT). It is used in a rail transit system which uses a high-voltage multi-level rectifier and a high-frequency isolement. Many experiments have been undertaken on different aspects of converters of this kind. Among the numerous topologies of SSTT, the most attractive one is the topology combining high-voltage cascaded inverters and DC-DC (DC: Direct current) converters. In this thesis, a new type of electric traction system based on SSTT is proposed on the basis of previous researchers.

1.1 Electric Traction

The traction system that uses electricity in all stages or some stages of a vehicle movement is referred to as an electric traction system. In an electric traction system the driving power to draw a train is generated by the traction motors. The electric traction system can be broadly divided into two groups: one is self-powered and the other one is third-rail system.

1.1.1 Types of Track Electrification Systems

The track electrification refers to the type of source supply system that is used while powering the electric locomotive systems. It can be AC or DC or a composite supply. Selecting the type of electrification depends on several factors like availability of supply, type of an application area, or on the services like urban, suburban and main line services, etc. The three main types of electric traction systems that exist are as follows:

- i. Direct Current (DC) electrification system
- ii. Alternating Current (AC) electrification system
- iii. Composite system.

II. PROBLEM IDENTIFICATION

The lack of scalability to higher voltage levels is a problem with typical SST configurations. As previously stated, today's SST topologies employ multilevel converters at the SST's input point, resulting in a high degree of modularity. In this application, the cascaded Dual-bridge multilevel converter is widely used, and the use of a diode clamped multilevel converter is also mentioned.

The lack of a High-Voltage DC (HVDC) terminal in most common SST configurations is another limitation that prevents SSTs that can be used in future DC distribution networks. Note that in common SST topologies, a Medium-Voltage DC (MVDC) connection usually has a voltage level of 25 kV or less and is unable to interface a DC distribution network. As a result, new SST topologies with the potential to interface a DC distribution network must be analyzed. An SST topology with both HVAC and HVDC terminals can be used in either AC or DC distribution networks, or it can connect to both networks at the same time and perform power routing. This topology can be used for any kind of distribution network/load/storage configuration if both LVDC and LVAC terminals are available.

- The HF/MF transformer in the DC-DC stage performs the same function as a traditional 50 Hz transformer: voltage transformation and electrical isolation of the HV and LV sides. High voltage and frequency operation, on the other hand, presents particular difficulties in transformer architecture.
- Since high-frequency processing increases core loss and temperature, choosing a magnetic material with a high saturation flux rate, low specific loss, and high operating temperature is critical for high performance and power density.
- Isolation requirements and thermal control must be closely considered since reduced volume and weight is a necessary feature.
- Skin and proximity consequences in the windings are greatly enhanced as compared to 50 Hz operation; thus, careful wire selection is needed.

- For optimum power transfer in the DC-DC stage, the core and winding configurations must be chosen based on thermal requirements and the leakage inductance criterion.

III. METHODOLOGY

3.1 Solid State Transformer basic concept

The basic solid-state transformer topology consists of three main sections: the first is the converter or converters, which is responsible for converting the line low frequency AC into the necessary high frequency AC, the second is the high frequency transformer, and the third section is the converter or converters, which is responsible for producing line frequency AC from the high frequency AC. The high frequency transformer separates the high and low voltage sides of the transformer by providing insulation between its terminals. A solid state transformer's basic structure is shown in Figure.

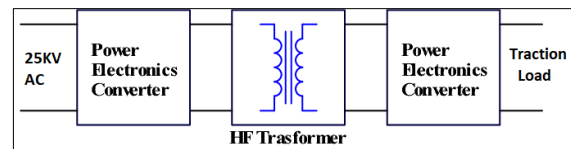


Figure 3.1: Generalized solid-state transformer circuit.

3.2 Solid State Transformer configurations

Many solid state transformer power topology equivalents can be found in the literature. They develop a method for classifying SST topologies and selecting the required configuration based on the needs. However, it's exciting to learn that all of those configurations can be categorized into four categories.

1. Single-stage with no DC link.
2. Two-stage with low voltage DC link (LVDC).
3. Two-stage with high voltage DC link (HVDC).
4. Three-stage with both high and low voltage DC links.

Figure 3.2 shows a graphical representation for all the previously stated classes to illustrate them. Insulated Gate Bipolar Transistors (IGBT) and high frequency transformers with high voltage ratings, such as those used in the distribution system are not readily available at the moment. A modular approach may be one of the solutions to these problems. The ripple of the current would also be reduced using the interleaving technique, resulting in a reduction in the size of the filter used to smooth the current.

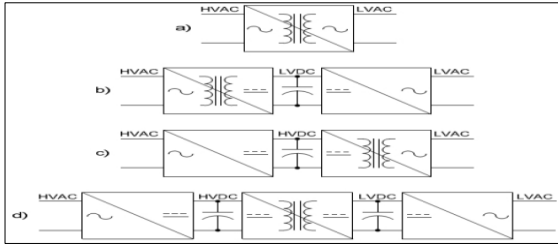


Figure 3.2: SST configurations: a) single-stage, b) two-stage_with_LVDC_link, c) two-stage_with_HVDC_link, and d) three-stage.

The three-stage SST architecture can be modeled as seen in Figure 3.2. It is made up of two semiconducting converter bridges linked by a single transformer in the middle. The first converter is wired to the MV side and transforms three-phase alternating current voltages with frequencies of 50 or 60 hertz to a DC voltage in the MV DC circuit. The MV-converter Bridge's second part then transforms the DC voltage back to AC, but at a faster speed. Because of the higher AC frequency, the magnetic properties of the transformer center are best used, and the transformer may therefore be made considerably smaller while maintaining the same power capacity. On the LV line, a second converter bridge transforms the high frequency AC voltage to DC and then to the same power frequency, 50 or 60 Hz. SSTs, as shown in Figures 3.2, use power electronic converters and a high frequency transformer to convert medium or high voltage on the primary side to low voltage on the secondary side. As a result, utilities now have greater grid power while being substantially smaller and lighter. It's worth noting that the same or very similar design can be used to produce a DC secondary-side waveform as well as a high-frequency AC waveform. These alternatives are not investigated in this analysis since neither the configuration nor the architecture depicted in Figure 3.3 can be substantially altered to accommodate them. This thesis' research is mainly concerned with a three-stage SST for interfacing MV and LV structures.

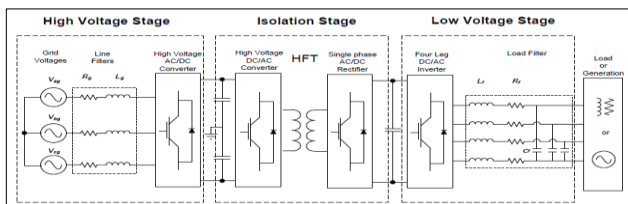


Fig. 3.3. Schematic configuration of a three-stage SST.

3.2.1 Description of Selected SST Topologies

To test the effect on the transformer, three SST topologies known as configuration (d) (see Fig. 3.2) are chosen. Three modules are paired in series on the HV side and parallel on the LV side in these topologies. The number of modules is determined by the voltage blocking power of 25 kV IGBTs, as used in the case study mentioned in section 4.2. AC-DC rectifiers switching at 1 kHz transform 440 V AC rms 50 Hz from the traction transmission line to three phase 25 kV HV DC connections in the selected configurations. As SSTs are connected to an LV DC grid, isolated bidirectional DC-DC converters with 1 kHz medium-frequency (MF) transformers decrease the voltage to 400 V DC (LV DC link). The selected SST topologies for the case study differ in their understanding of the DC-DC converter stage, resulting in different voltages applied to the transformers, resulting currents, and leakage inductance specifications for optimum power transfer. As a result, each topology would necessitate its own transformer architecture. The topologies are as follows: (I) full bridges on both HV and LV sides, (II) half bridges on both HV and LV sides, and (III) half bridges on both HV and LV sides as seen in Figs. 3.4, 3.5, and 3.5, respectively. When S1p and S4p are allowed in topology (I), the voltage across the primary winding of the transformer, VT1, equals the voltage in the HV DC connection, V1, resulting in $VT1 = V1$. V1 is the product of S2p and S3p both being on VT1. As S1s and S4s are switched on, the voltage in the secondary winding of the transformer, VT2, equals the voltage in the LV DC link, V2, resulting in $VT2 = V2$ and $VT2 = V2$ when S2s and S3s are turned on. As a result, in a full-bridge converter, the voltage applied to the main and secondary of the transformer is equal to the HV and LV DC links, respectively.

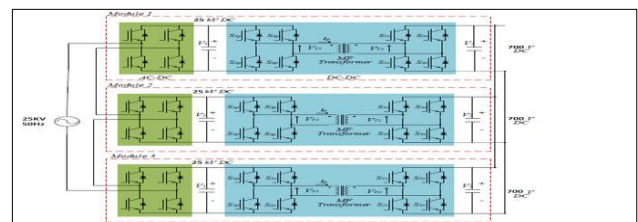


Figure 3.4 SST topology with full bridges on HV and LV sides (I)

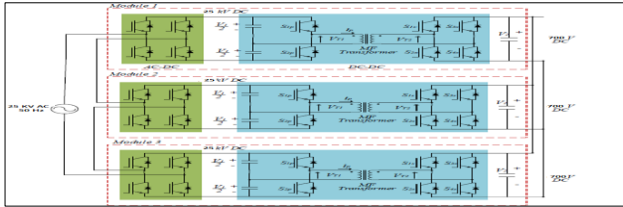


Figure 3.5 SST topology with half bridges on HV side and full bridges on LV side (II)

Topology (II) uses a half-bridge converter on the HV side, meaning that 2 transistors are replaced by two condensers opposed to one full-bridge converter. The voltage applied to the transformer on the main side now represents half the overall voltage of the DC, while $V_{T1} = V_{T2}$. The current through the main winding and switching units of the transformer is twice as high as the total bridge at the same power rating.

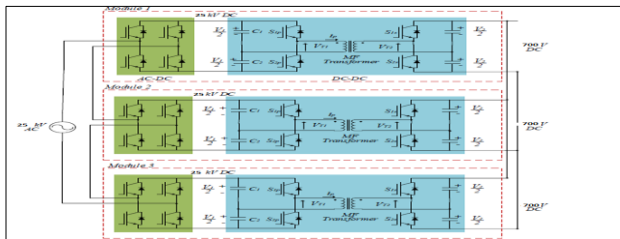


Figure 3.6 SST topology with half bridges on HV and LV sides (III)

High bridge (III) converters are used at HV and LV ends, which means $V_{T1} = V_{T2}$ is used on the main side and $V_{T2} = V_{T1}$ on the secondary side. In topology, half bridge converters are used on both sides. The main and secondary currents are twice as high as the topological currents (I).

3.2.2 Operating Principle of the DAB

The DC-DC converter point, which is created by a DAB, can be simplified by the reference to the secondary bridge as the primary end and by defining the transformer with its leakage inductance L_k . Since the magnetizing inductance can be much greater than that of the leakage, the magnetizing branch may be referred to as an open circuit. The transformer leakage inductance is the main energy storage and transfer component.

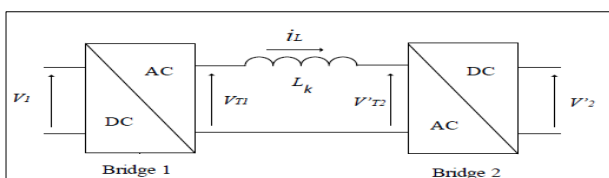


Figure 3.7 Simplified representation of a DAB

The phase change between the primary and secondary voltages defines the voltage. Another modulation scheme introduced in the literature is the hybrid phase shift and pulse broadness modulation. This modulation has certain benefits over traditional phase shift modulation (PSM). The PSPWM solution reduces transformer rms thus widening the zero-voltage transfer (ZVS) operating range for large differences in input and output voltage. The theoretical working waveforms of the DAB with the PSM is seen in Fig. 4.8 where $\theta = \omega t = 2\pi f_{sw}t$, is the frequency of switching, β is the current inductor angle of the i_L zero-crossing, μ is the phase-shift angle, and i_p is the main current. In case that $V_{T1} > V_{T2}$ then power is passed from Bridge 1 to Bridge 2 theoretical wave forms can apply on each of the chosen SST topologies.

In fig. 3.8, each mode of operation is seen by a switching system status change that results in six modes in one loop. Since each half cycle of the switching frequency is replicated due to symmetry the present waveform needs that only coefficients of an inductor current for cycles between modes 1 and 3 are determined for i_L 's dynamics. The anti-parallel Dxx diodes and driving intervals at all intervals.

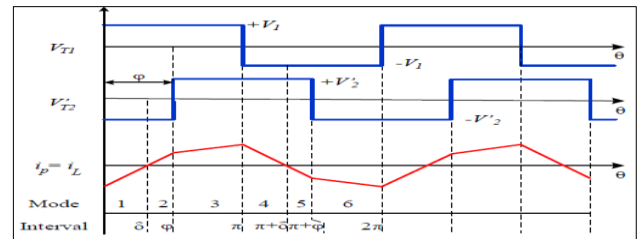


Figure 3.8 Theoretical operating waveforms of a DAB

3.2.3 Magnetic Core Characterization

The properties of the magnetic materials are also important to consider. In particular, a core material suitable for a specific application may be characterized with four measures: core failure densities (Pfe), saturation density flux (Bsat), relative permeability (μ_i), and curie temperature (T_c). Ferrite, silicon steel, amorphous, and nano-crystalline are typical core magnetic materials used for high-frequency transformers. Table lists a distinction of chosen magnetic materials for the above properties. Ferrite material is widely used for high frequency applications because the core density and low cost are very low, but it has a lower saturation flux density (~ 0.4 T) resulting in the use of a large and heavy-duty transformer. Additionally, a higher densities saturation flux (~ 1.5 t), high permeability and high temperature of the silicon steel content is ideal for high-power applications.

Where A_e represents the effective transversal core field, N represents the number of flips, T represents the time, and D represents the voltage waveform operating period. The equation was used to calculate the arousal voltage used to maintain a flux density of 0.1 T under various excitation conditions (i.e., different frequencies and duty cycles). The themesis indicate that lower losses were achieved at 50 percent duty cycles and that when $D = 50$ percent, $f = 100$ kHz and $B = 0.1T$ were chosen from Fig.4.8, ferrite 3C94 material responded with approximately eight times higher losses than Nano-Crystalline 500F, while the amorphous 2605SA1 loss is 1,5 times higher than that of nano-crystalline Vitroperm 500F. These results correspond with the measured iGSE values.

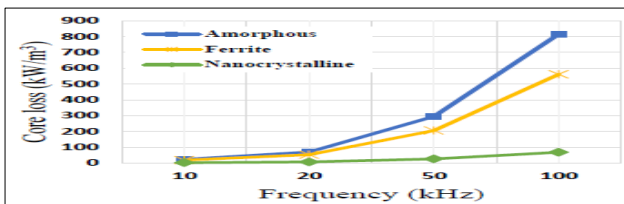


Figure 3.13 Core losses of selected materials under different frequencies, $D=50\%$, and $B=0.1T$

IV. HIGH-FREQUENCY TRANSFORMER DESIGN METHODOLOGIES

In contrast to the flux density optimization criterion, the proposed design solution includes design issues discussed regarding HF effects of the center and winding as well as conditions for separation and leakage induction. The definition flowchart that has been applied in MATLAB® is depicted in Fig. 3.17. The overview of each design process is shown below.

- Step 1. System and Topology Specifications
- Step 2. Material Properties
- Step 3. Optimum Flux Density
- Step 4. Core Dimensions
- Step 5. Winding Characterization
- Step 6. Isolation Distance
- Step 8. Volume Calculation
- Step 9. Losses Calculation
- Step 10. Efficiency and Temperature Rise

V. RESULT AND DISCUSSION

The simulation results from two sections of the system are presented in this chapter.

The system's first component is a stand-alone SST with a model that accounts for semiconductor losses. The system's second component is the electrification of the traction drive system, which is connected to an SST.

5.1 Results come out from Stand – alone SST

This section presents transformer design examples realized with the proposed design methodology implemented in the developed MATLAB® program.

5.1.1 Design SST: 5 MVA, 1 kHz, 25KV / 1000 V, core-type transformer

The transformer architecture builds on chapter 1's case study on the topology of the SST. The architecture consists of a central transformer of 5 MVA, 1 kHz operating frequency and a 25 kV-1000 V voltage rate. The following steps are listed for the design of the transformer:

Step 1. System and Topology Specifications

- Expected-Efficiency, $\eta \geq 98\%$
- Rated-output-power, $P_{out} = 5\text{-MVA}$
- Secondary-voltage, $V_s = 1000\text{-V}$
- Primary-current, $I_p = 100\text{-}115\text{-A}$
- Secondary-current, $I_s = 807.5\text{-A}$
- Frequency, $f = 1\text{-kHz}$
- Ambient-temperature, $T_a = 30\text{-}^{\circ}\text{C}$
- Duty-cycle, $D = 0.5$
- Waveform-factor, $k_f = 4$
- Expected-temperature-rise, $\Delta T = 70\text{-}^{\circ}\text{C}$
- Leakage-inductance, $L_{lk} = 8\text{-mH}$
- Window-utilization-factor, $k_w = 0.4$
- Isolation-voltage, $V_{ins} = 95\text{-kV}$
- Primary-voltage, $V_p = 25000\text{-V}$

Step 2. Material Properties

The substance picked is 2605SA1 amorphous whose parameters are removed by Steinmetz. NOMEX with a dielectric power of 27 kV/mm is a chosen insulating material with a protection margin of 40%.

Step 3. Optimum Flux Density

The estimated optimal flow density is $B_{opt} = 0.3$ T. This value is below the saturation flux density $B_{sat} = 1.56$ T and is designed because this particular system needs a high performance.

Step 4. Core Dimensions

The measured area product is $A_p = 22976$ cm⁴. The core AMCC-1000 is the broader chosen core with a surface product of 966 cm⁴; thus, 24 cores must always be stacked to complete the surface product.

This design has a shell type, which is also specified in the software, for the desired transformer design. Chapter 4 discusses the proportions of the chosen heart.

Step 5. Winding Characterization

Present densities of $J = 107.98 \text{ A/cm}^2$ estimated by (4-6). The main and secondary bare wire areas needed for these current densities are $A_{wp} = 0.7871 \text{ cm}^2$ and $A_{ws} = 7.4779 \text{ cm}^2$, respectively. The skin depth is $\mu = 0,1209 \text{ cm}$ at 3 kHz; therefore the Litz wire chosen must contain strands of 0,0459 cm^2 maximum surface area. The strand size chosen is #18AWG with an area of $0.8046 \times 10^{-3} \text{ cm}^2$ and a resistivity of $209.5 \mu \text{ liters}$ at 20°C . The resistivity is calibrated to the maximum working temperature of 100°C , resulting in a temperature of $275.37 \mu/\text{cm}$. The minimum number of strands is $PS = 96$; for the build a custom Litz wire #18 AWG/100 is chosen. For secondary winding, so for a limit of 1,000 wires, the same wire dimension can be used. The number of primary turns is determined with $N_p = 11$, after the wire has been picked. $N_p = 18$ and the number of secondary turns $N = 2$ was used to maximize the leakage.

Step 6. Isolation Distance

The material insulation was defined in phase 1, and the minimum insulating distance measured between windings was reduced = 8.8 mm. This is a free parameter that can be changed to meet the requirement of leakage induction in the next step.

Step 7. Leakage Inductance Estimation

The leakage inductance is estimated to be $L_k = 8 \text{ mH}$. After several iterations, the chosen isolation distance is $d_i = 35 \text{ mm}$, resulting in $L_k = 8 \text{ mH}$.

Step 8. Volume Calculation

$L_k = 8 \text{ mH}$ is the leakage latest estimate. After multiple iterations, the separation distance selected is $d_i = 35 \text{ mm}$, which corresponds to $L_k = 8 \text{ mH}$.

Step 9. Losses Calculation

For the selected parameters, the core loss is $\square\square\square = 2.281 \text{ kW}$ and the winding loss is $\square\square\square = 0.313 \text{ kW}$; thus, the total transformer loss is $\square\square = 2.594 \text{ kW}$.

Step 10. Efficiency and Temperature Rise

The estimated efficiency of the transformer is therefore $\alpha = 98.7\%$ which corresponds to the desired efficiency stated in phase 1. The predicted temperature rise is $T = 88^\circ \text{C}$ if normal convection is taken into consideration.

Since this value exceeds the expected temperature increase previously established, a proper cooling system is needed to meet this requirement. If not, the artist should choose a heart that is bigger. The transformer performance and scale are optimized for the selected parameters. In addition, the inductance required to pass maximum power with the DAB was added to the transformer leakage inductance, avoiding the need of an external inductance. The outcome of the Matlab machine simulation.

The SST should play a major role in replacing traditional low-frequency transformers.

Following are the major disadvantages of traditional iron and copper transformers:

- Designs are large and heavy, and
- Where mineral oil spills, environmental issues arise,
- Voltage decrease under load,
- Inability to decrease flickering;
- Harmonic sensitivity;
- Inability to transform single-phase operation to three phase power supply for certain types of machine;
- No power storage capacity;
- Unwanted voltage properties (e.g. tension sags, failures) at one side propagated to the other, •
- Inability to decrease under the offset loading,
- Conventional transformer losses at average load level is comparatively high: transformers show optimum performance at nominal load when the average load level for delivery transformers was around 30%.
- Compared to traditional transformers, the major advantages of SSTs are:
- Quick management of bidirectional active flow of electricity, • Enhanced energy efficiency,
- Easy resource incorporation,
- Correction of power,
- Reactive power control on both SST sides,
- Fault separation of main and secondary sides
- Instant voltage adjustment.
- However, in front of the traditional transformer, the SST often has some disadvantages; the following could include:
- The cost of the SST is greater than its standard equivalent of the transformer. It then becomes apparent that the convenient transformer requires inexpensive and efficient high-voltage semi-conductors to compete with it.
- The SST is more advanced (i.e. requires more design equipment and components) than the traditional transformer due to to semiconductor losses, which increases somerisks in terms of performance and reliability.

- The SST shows higher EMIs than the traditional transformer, so that the effects of SST can be understood better and the influence can be reduced better.

5.2 Results come out from SST based 3 phase I/M Traction Drive

For several purposes, the solid state transformer SST may be able to replace the traditional line frequency transformer (conventional transformer) in railway traction applications:

SST decreases the size and weight of the transformer system as compared to traditional transformers, which are large and bulky. The train's output will improve as the power density increases. The new traditional transformer is designed to provide the most power per pound of weight. However, due to other main parameters, the average efficiency is about 92 %. The SST can improve a transformer's efficiency by up to 98%.

For traction applications, the SST requires special design:

- Be compact both in size and weight;
- High tolerance with vibrations and shocks;
- Multiple windings (output windings contain auxiliary windings);
- Relatively high short-circuit impedances and high reliability levels;

5.3 Simulation and waveform performance

Simulation and their waveform performance of the SST based 3 phase induction motor traction drive with PI control strategy. The choice of 25 kV was related to the efficiency of power transmission as a function of voltage and cost, not based on a neat and tidy ratio of the supply voltage. For a given power level, a higher voltage allows for a lower current and usually better efficiency at the greater cost for high-voltage equipment. It was found that 25 KV was an optimal point, where a higher voltage would still improve efficiency but not by a significant amount in relation to the higher costs incurred by the need for larger insulators and greater clearance from structures.

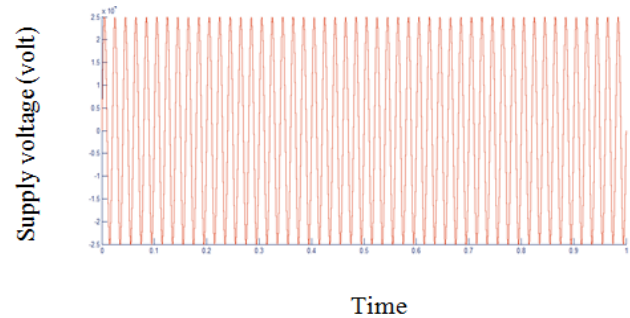


Fig. 5.1 Supply Voltage 1 phase 25 KV 50 Hz AC form pantograph

Fig. 5.1 shown a high-voltage 25 KV AC 50 Hz from catenary transmission line fed with cascaded converter through out of pantograph. A power supply system for railway traction applications with a multilevel AC/DC converter is the subject of this Simulink disclosure. The transformer can operate at frequencies lower than 1 kHz and higher than the AC line frequency. More than one parallel-connected secondary converter is provided on the secondary side of the transformer and is connected to a DC connection. The multilevel AC/DC converter can continue to operate with reduced power delivery if one of the secondary converters fails.

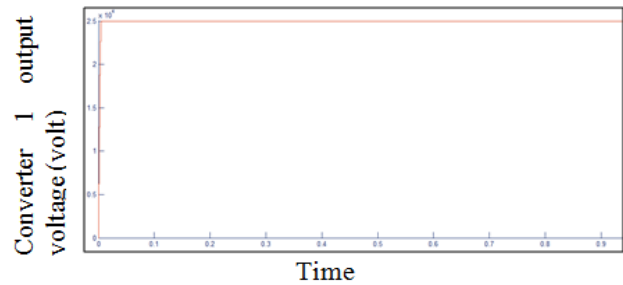


Fig. 5.2 Converter 1 output 25KV DC Voltage

In this research, we first described the Solid State Transformer's system functionality, followed by the proposed system configuration with various levels of control for the configured system to meet the required functionality in the later sections of the section. Fig. 5.3 and Fig. 5.4 are shown output of 1 KHz solid state transformer about 700 V AC voltages and Converter 2 output 700 KV DC Voltage irrespectively.

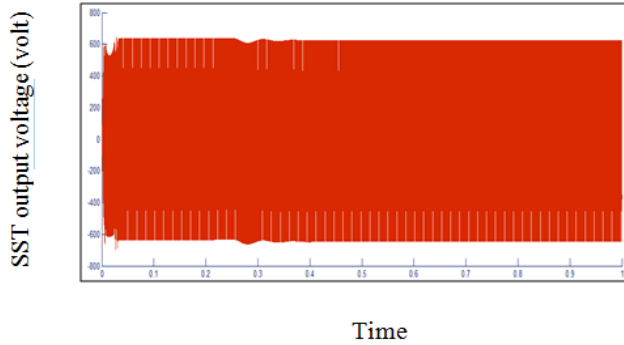


Fig. 5.3 SST output 700 KV AC Voltage 1000Hz

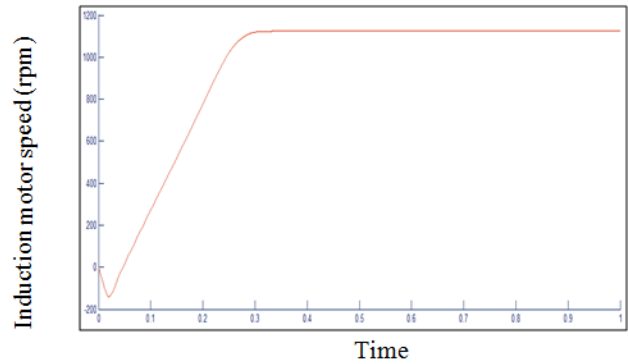


Fig. 5.7 Speed of 3 phase IM traction drive

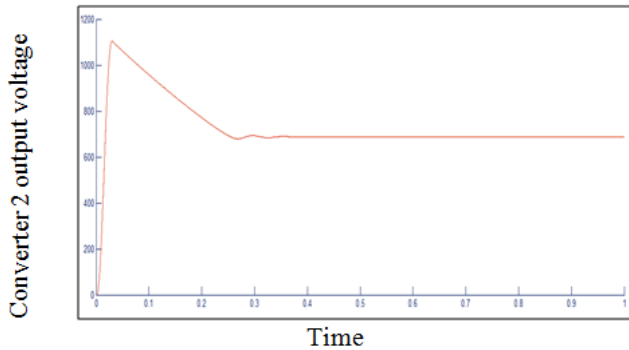


Fig. 5.4 Converter 2 output 700 KV DC Voltage

In propulsion systems, traction inverters are important for converting a 700V DC supply to a 440V 50 Hz AC supply. This Simulink section focuses on major design aspects of high voltage traction inverters, such as comparing various types of existing inverter topologies, analyzing power requirements in commercially produced modern electric traction, and addressing advanced power module packaging technology. Fig. 5.6 is shown output voltage and current of Inverter 2 irrespectively.

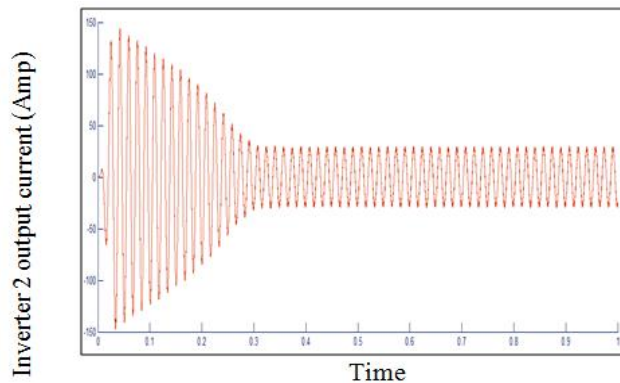


Fig. 5.6 Inverter 2 output 30 A AC 50 Hz Current

This simulation describes the operation of the VSI and pulse converter in DC-fed and AC-fed railway traction drives with three-phase induction motors. The accompanying motor control scheme affects the dynamic output of VSI-fed drives; this arrangement is described: vector control with pulse-width modulation (PWM) and a PI controller-based direct voltage frequency (v/f) self-control system. The performance of speed in rpm about 1200 rpm was shown in Fig. 5.7.

VI. CONCLUSION AND FUTURE SCOPE

6.1 Conclusions

The SST is an enabling technology for future energy systems and applications characterized by space constraints due to its availability of functionalities such as power flow control, voltage management, and harmonics suppression, voltage sag ride through capability, and volume and weight reductions.

The main desired characteristics on an SST topology are: availability of an LV DC link, modularity capability, unidirectional or bidirectional power flow control functionality, reduced number of components, and soft switching operation. In the research it is explained why topologies consisting of an active-front-end rectifier stage (AC-DC), a DC to DC stage with a HF or MF transformer, and a back-end inverter stage (DC-AC) have been proposed the most for SST applications and considered for the selected case study.

To evaluate the case study, three SST topologies were selected in particular. Topology (I) has complete bridges on both the HV and LV sides, topology (II) has half bridges on both the HV and LV sides, and topology (III) has half bridges on both the HV and LV sides.

Various topologies have been identified which cause different current and voltage stresses on the HF/MF transformer, affecting the requirements for insulation. For example, the transformer's stress voltage was 25 kV; for topology (II) and (III) a stress of 1 kV was applied at the same power level. The HF transformer can, however, comply with international delivery transformer requirements. For eg, an isolation level of 25 kV for the case study should be considered in light of the isolation criterion. In addition, each topology resulted in different leakage inductance requirements for maximum power transfer in the DC-DC converter stage. The leakage inductance for topology (I) was 8.01 mH; while for topology (II) and (III) were 0.63 mH and 0.71 mH, respectively.

As a result, it is recommended that the transformer design provide a leakage inductance specification to prevent the need for an additional inductor to achieve the necessary inductance, which may result in a lower power density. The four design considerations were investigated in order to establish the basics for the proposed HF/MF transformer design:

- Core material selection
- HF effects in core and windings
- Isolation requirement
- Leakage inductance integration

A magnetic core characterization was provided for four magnetic materials: ferrite, silicon steel, amorphous, and nanocrystal line, in terms of core material selection. They are not recommended for the considered application due to the ferrite's low saturation flux density and the nanocrystal line material's high manufacturing cost. As a result, amorphous materials with high saturation flux density and low core-loss density, as well as silicon steel with thin laminations to reduce eddy current losses, are the best choices for distribution. The i2GSE, proposed in, takes into account the relaxation effects in the magnetic material during zero-voltage conditions, making it more reliable for low duty cycles (D 0.2) than the iGSE. Experimental findings reported in this study confirmed the iGSE's inaccuracies for low duty cycles, where the two-winding approach was chosen for core loss measurements. The use of so-called Litz wire for the windings eliminates HF effects in the windings (i.e., skin and proximity effects). With a BIL of 95 kV, the corresponding isolation distance for the case study was 16 mm. This distance can also be used as a free parameter to set the leakage inductance of the transformer to the desired value for optimal power transfer.

These design factors were implemented into the proposed transformer design methodology outlined in

REFERENCES

- [1] Thiago Parreiras, Fernando Amaral and Gideon Lobato, "Forward Dual-Active-Bridge Solid State Transformer for a SiC-Based Cascaded Multilevel Converter Cell in Solar Applications", IEEE Industry Applications Society, IEEE 2018.
- [2] Pares P. Luhana and Apurva N. Christian, "Solid state transformer controller and its interfacing with Electric Railway Traction based distribution systems", International Conference on Energy, Communication, Data Analytics and Soft Computing (ICECDS), IEEE 2017.
- [3] Sreedhar Madichetty, Bhanu Duggal, Aumkar Borgeonkar and Sukumar Mishra, "Modeling and design of solid state transformer for microgrid", IEEMA Engineer Infinite Conference (eTechNxT) IEEE 2018.
- [4] Vijayakrishna Satyamsetti, Andreas Michealides and Antonis Hadjiantonis, "Forecasting on solid state transformer applications", International Conference on Intelligent Sustainable Systems (ICISS) IEEE 2017.
- [5] Felix Rojas, Matias Diaz, Mauricio Espinoza and Roberto Cárdenas, "A solid state transformer based on a three-phase to single-phase Modular Multilevel Converter for power distribution networks", Southern Power Electronics Conference (SPEC) IEEE 2017.
- [6] Umar Khalid, Muhammad Mansoor Khan, Zihang Xiang and Yu Jianyang, "Bidirectional modular Dual Active Bridge (DAB) converter using multi-limb-core transformer with symmetrical LC series resonant tank based on cascaded converters in solid state transformer (SST)", China International Electrical and Energy Conference (CIEEC) IEEE 2017.
- [7] Harish Sarma Krishnamoorthy, Prasad Enjeti and Jose Juan Sandoval, "Solid State Transformer for Grid Interface of High Power Multi-Pulse Rectifiers", IEEE Transactions on Industry Applications IEEE 2017.
- [8] H. D. Awasty, "Railway electrification in India", Proceedings of the Institution of Electrical Engineers, IEEE 1964.
- [9] Walter Lhomme, Philippe Delarue and Tiago Jose Dos Santos Moraes, "Integrated traction / charge / air compression supply using 3-phase split-windings motor for electric vehicle", IEEE Transactions on Power Electronics, IEEE 2018.
- [10] N. V. V. R. Kumar, P. V. Rajgopal, S. N. Saxena, S. K. Mondal, B. P. Muni and J. V. R. Vithal, "A new GTO-based single-phase to three-phase static converter for loco auxiliaries", Proceedings of International Conference on Power Electronics, Drives and Energy Systems for Industrial Growth, IEEE 1996.
- [11] Laxman Singh, Chandan Vaishnav and Vivek Shrivastava, "Performance Analysis of Hybrid Network of Indian Traction Power System Using Renewable Energy Sources" 2016 International Conference on Micro-Electronics and Telecommunication Engineering (ICMETE), IEEE 2016.
- [12] Sharvari Sane; Swati Sharma; Sanjay K Prasad, "MATLAB based model for internal electrification system of local trains" 2016 International Conference on Communication and Signal Processing (ICCCSP), IEEE 2016.



International Journal of Recent Development in Engineering and Technology
Website: www.ijrdet.com (ISSN 2347-6435(Online) Volume 10, Issue 8, August 2021)

- [13] S Srinivasan, A.K. Parvathy and P. Deivasundari, "Dual active bridge — A good candidate for solid state transformer", IEEE International Conference on Power, Control, Signals and Instrumentation Engineering (ICPCSI) IEEE 2017.
- [14] E. R. Ronan, S. D. Sudhoff, S. F. Glover, and D. L. Galloway, "A power electronic-based distribution transformer," IEEE Transactions on Power Delivery, IEEE 2002.
- [15] J. W. Kolar and G. Ortiz, "Solid-State-Transformers: Key Components of Future Traction and Smart Grid Systems," IEEE International Power Electronics Conference - ECCE Asia, IEEE 2014.
- [16] W. McMurray, "Power converter circuits having a high-frequency link" U.S. Patent, IEEE, 1970
- [17] Xu She, R. Burgos, Gangyao Wang, Fei Wang, and A. Q. Huang, "Review of solid state transformer in the distribution system: From components to field application," IEEE Energy Conversion Congress and Exposition (ECCE), IEEE 2012.
- [18] Jianjiang Shi, Wei Gou, Hao Yuan, Tiefu Zhao, and A. Q. Huang, "Research on voltage and power balance control for cascaded modular solid-state transformer," IEEE Transactions on Power Electronics, IEEE 2011.
- [19] D. Dujic, F. Kieferndorf, Francisco Canales, and U. Drogenik, "Power electronic traction transformer technology," 7th International Power Electronics and Motion Control Conference (IPEMC), IEEE 2012.
- [20] T. Zhao, G. Wang, S. Bhattacharya, and A. Q. Huang, "Voltage and Power Balance Control for a Cascaded H-Bridge Converter-Based Solid-State Transformer", IEEE Transactions on Power Electronics, IEEE 2013.
- [21] R. K. Gupta, K. K. Mohapatra, and N. Mohan, "A novel three-phase switched multi-winding power electronic transformer," IEEE Energy Conversion Congress and Exposition, IEEE 2009.
- [22] Kaushik Basu, R. K. Gupta, S. Nath, G. F. Castelino, K. K. Mohapatra, and N. Mohan, "Research in matrix-converter based three-phase power electronic transformers," International Power Electronics Conference, IEEE 2010.
- [23] J. Venkat, A. Shukla, and S. V. Kulkarni, "A novel dq-vector based control for the three phase active rectifier in a power electronic transformer," Annual IEEE India Conference, IEEE 2013
- [24] J. Huber and J. W. Kolar, "Common-Mode Currents in Multi-Cell Solid-State Transformers," International Power Electronics Conference - ECCE Asia, IEEE 2014.
- [25] Xinyu Wang, Jinjun Liu, Taotao Xu, Xiaojian Wang, and Liansong Xiong, "Control of a three-stage three-phase cascaded modular power electronic transformer," IEEE Applied Power Electronics Conference and Exposition (APEC), IEEE 2013.